29th Congress of the International Council of the Aeronautical Sciences
St. Petersburg, Russia; September 7-12, 2014

AERODYNAMICS AND FLIGHT DYNAMICS PROBLEMS OF HIGH SPEED VEHICLES AND WAYS FOR THEIR SOLUTION

Efremov A.V., Popov S.A., Nikitchenko I.A., Koshelenko A.V., Tiumentzev Y.V.
Moscow aviation institute

Keywords: *flight dynamics, control system, aerodynamics*

Abstract

The flight control system design is carried out with the goal to provide the best dynamics response and necessary stability in all flight envelope with taking into account the specific peculiarities of the considered vehicle. As a rule the dynamics of a novel vehicle is characterized by the new dynamic peculiarities. Their deep knowledge guarantees the best solution for their suppression by corresponding selection of airframe configuration and flight control system (FCS).

One of the new type of vehicle developed recently is the high speed vehicle (HSV) with the ramjet. All these vehicle can be divided on two types of configurations: wave riders (X-43A, X-51A, USA) and symmetrical: Hifire (Australia), X-90 (Russia).

Their design required to solve many problems in aerodynamics, thermodynamics, propulsion, materials. Basically these problems were solved in the initial stage of the hypersonic vehicle design. The following stage exposed the problems of these vehicle in other aspects, in particular, in flight dynamics and control. A number of researches were carried out in these area [1]-[7] what allow to develop the control systems for realization of their mission.

The investigations considered in the paper generalize the results of researches carried out by authors in this area during the last period.

The following aspects of flight control system design and flight dynamics of HSV are considered in the paper:

- *Peculiarities of HSV flight dynamics,*
- *Estimation of HSV aerodynamic and thrust forces,*
- *Flight control system design.*

1 Peculiarities of HSV flight dynamics

1.1 Peculiarities in aerodynamic and thrust force characteristics

Possible instability in different control channels.

The analyze of hypersonic vehicle developed in USA (X-43A, X-51A, NASP) and experience in evaluation of aerodynamics characteristics of the other hypersonic configurations demonstrated the possible static unstability in different channels [4]. As for X-43A the longitudinal instability takes place at high angle of attack or Mach numbers. (fig 1)

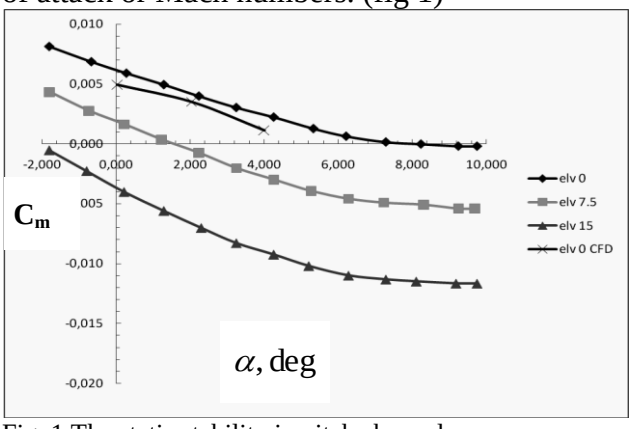

Fig. 1 The static stability in pitch channel

Nonlinearities of aerodynamic and thrust force characteristics

Nonlinearities of aerodynamic characteristics are the typical feature of HSV.

The increase of sideslip β, angle of attack and Mach number caused the exposition of nonlinear aerodynamic characteristics. The typical dependences of α and M on coefficient C_n are shown on fig. 2

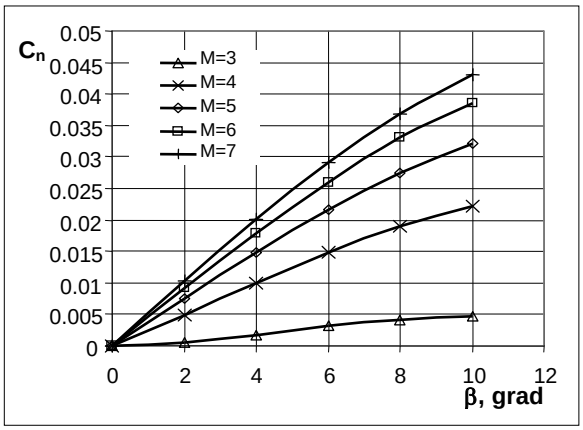

Fig. 2 The lateral static instability

Estimation of the thrust force (T) demonstrated the considerable dependence of angle of attack on it. This nonlinearity is typical in the range of angle of attack characterizing the cruise flight (fig. 3)

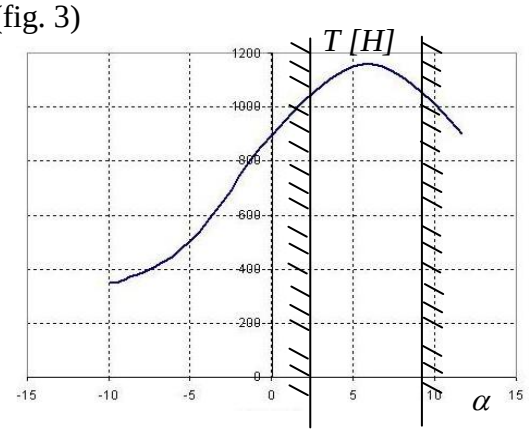

Fig. 3 The dependence of thrust $T = f(\alpha)$

These results lead to the conclusion necessity to know precisely the aerodynamic characteristics for the following mathematical modeling and development of highly augmented flight control system for suppression of instability and nonlinear effects.

Considerable coupling between thrust and aerodynamics forces.

This peculiarity is the typical for high speed vehicle with wave rider configuration. Such configuration is highly integrated with the engine.(fig 4)

Fig. 4 Integration of ramjet and HSV fuselage

Its nose part takes place of a compressor and a tail part is the additional part of a nozzle. Because of this peculiarity the change of angle of attack leads to the change of shock waves at the inlet what causes the change of thrust force (fig. 3). At the same time the change of thrust changes the lift force created at the tail part of the vehicle. It changes the pitch moment and as a consequence - angle of attack (fig. 5). Because of very complicated mathematical models of these coupling effects it is very difficult to predict the thrust and aerodynamic characteristics accurately. Such uncertainty has to be taking into account in flight control system design.

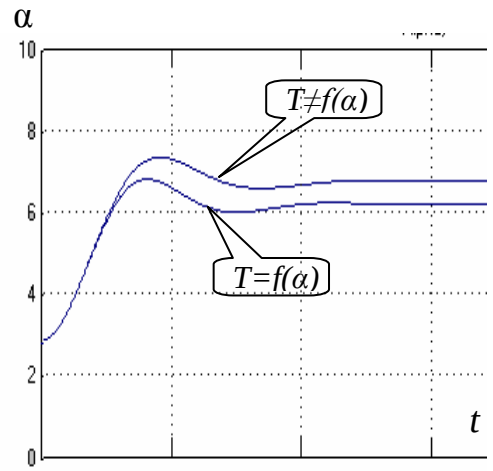

Fig. 5 Influence of thrust on angle of attack

1.2 Dynamics peculiarities of HSV

Considerable influence of air density on path motion.

As a rule the airplane path and angular motions are analyzed supposing the constant air density

(p=const). The more accurate simulation conducted for the case p≠0 demonstrated that the results of the simulation of angular motion are approximately the same for the both cases and are differed considerably for the simulation of the HSV path motion (fig.6)

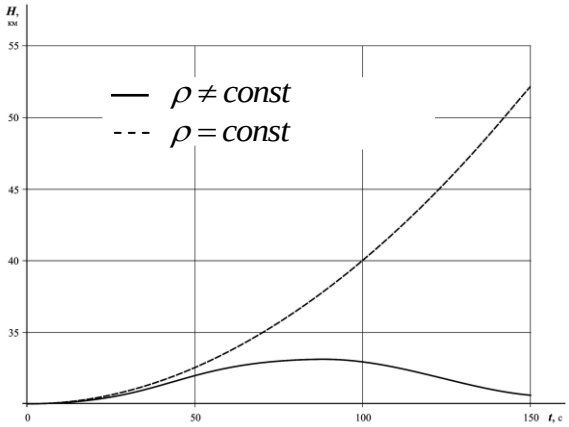

Fig.6 Influence of air density on path motion

Significant delay of the path motion. The path motion ($\gamma(t)$) is characterized by the time delay in comparison with the pitch time response $\theta(t)$. For the subsonic and supersonic aircraft such time delay is usually 1-3 sec. As for HSV it is higher at least 10 times. It means that these vehicles are extremely sluggish in path motion and it is very difficult to correct their trajectories.

High dynamics pressure (especially during the decent). Because of extremely extended flight envelope (fig. 7) some of flight regimes are characterized by the high dynamic pressure causing high short period frequency (up to 20-40 1/sec), low damping and high hinge moments. The typical pitch angle (a) and angle of attack frequency (b) response characteristics for the different *M* are shown on fig 8.

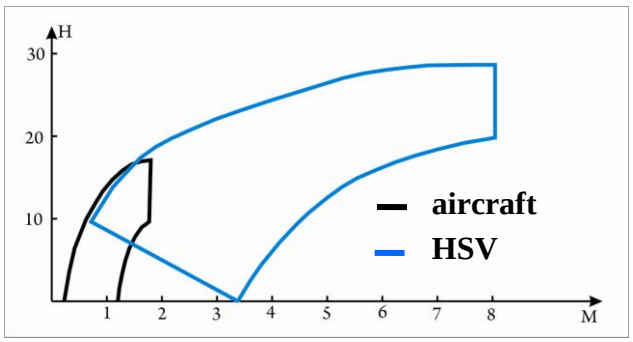

Fig. 7 HSV flight envelope

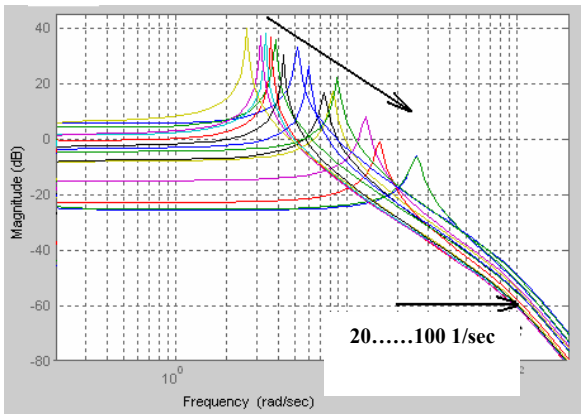

a.

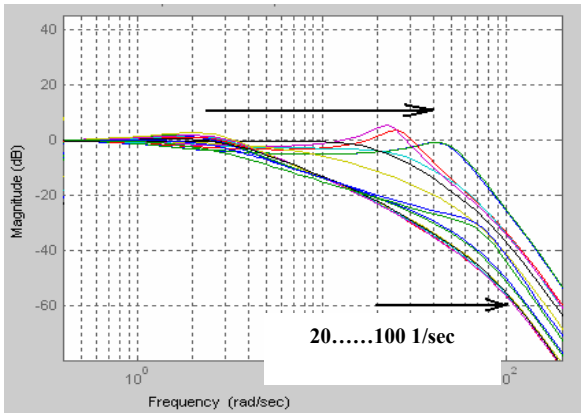

b.

Fig. 8 Typical pitch rate (a) and angle (b) of attack frequency response characteristic of HSV with FCS

The mentioned above peculiarities lead to necessity to develop the actuators with the band-width up to 100 1/sec and higher.

Influence of flexibility on HSV dynamics. The high short period frequency of HSP leads to the situation when ω_{sp} is close to the actuator frequency and to frequency (ω_f) characterizing the resonant peak in the spectral density $S_{nn}(\omega)$.

It is known effect that location of the frequencies ω_{sp}, ω_a and ω_f in close range might cause the problem of stability. It might take place for the large size HSV.

1.3 Estimation of the aerodynamic and thrust forces

Moscow aviation institute has a number of facilities for estimation of HSV aerodynamic characteristics.

There are the wind tunnels for the experimental tests:

-Supersonic wind tunnel with cross section 0.6x0.6 m, with the ranges of Mach number 0.6 ÷ 2.5. M and Re number $0.2 \cdot 10^6 \div 1.5 \cdot 10^6$

-Hypersonic wind tunnel with the working section 0.36x0.226x0.2 m, diameter of haggle 0.1 m, Mach number 2÷7 M.

Except it the aerodynamics department has the computer cluster T-Platform for calculation of characteristics:

32 processor Intel Xeon 5300 (64 cores)

Peak performance 966 Gflops.

The estimation of aerodynamics forces is carried out by use of two kinds of software:

- "Newton+", developed et MAI and used for preliminary estimation
- "ANSYS Fluent" used for verification.

During the research there were estimated several configurations. As a result the 9960 points were calculated corresponding to 25 different velocities and altitudes, 11 angles of attack, 6 angles of sideslip, 6 angles of elevator and rudder. All these results allowed to get the approximations

$(C_D, C_L, C_y, C_m, C_n, C_e) = f(\alpha, \beta, M...)$

necessary for the investigation of HSV dynamics. As an example the approximation for drag coefficient is shown below:

$$C_D(M,\alpha,\beta,\delta_a,H) = C_{D0}(M) + C_{Di}(M,\alpha) + C_{Di}(M,\beta) + \Delta C_D(M,\alpha,\delta_a) + \Delta C_D(M,\beta,\delta_a) + \Delta C_D(M,H)$$

$$C_{D0}(M) = 0.187 - \frac{0.072}{\sqrt{M}} + \frac{0.24}{M}$$

$$C_{Di}(M,\alpha) = a_1(M)\alpha + a_2(M)\alpha^2$$

$$C_{Di}(M,\beta) = b_1(M)\beta + b_2(M)\beta^2$$

$$a_1(M) = d_1 + \frac{d_2}{M} - \frac{d_3}{M^3}$$

$$a_2(M) = d_4 + \frac{d_5}{M} - \frac{d_6}{M^3}$$

$$b_1(M) = e_1 - \frac{e_2}{M}$$

$$b_2(M) = e_3 + \frac{e_4}{M}$$

$$\Delta C_D(M,\alpha,\delta_a) = f_1\left[\delta_{al}^2 + \delta_{ar}^2 + \alpha(\delta_{al} + \delta_{ar})\right]$$

$$f_1 = f(M)$$

$$f_2 = f(M)$$

$$\Delta C_D(M,\beta,\delta_r) = f_2\left[\delta_{rr}^2 + \delta_{re}^2 + \beta(\delta_{rr} + \delta_{re})\right]$$

$$\Delta C_D(M,H) = 25 \cdot \frac{1.8 \cdot 10^{-5} H + 1.5 \cdot 10^{-6} H^2}{\sqrt{M}}$$

Where:

$d_1, d_2, d_3, d_4, d_5, e_1, e_2, e_3, e_4, e_5$ - are the parameters of approximation

α, β - angles of attack and sideslip

M- Mach number

δ_a - elevon deflection

"l"- left, "r" – right

δ_r - rudder deflection

"l"- left, "r" – right

H – altitude [km]

As an example the calculated and shown on fig. 9 dependence $C_L = f(\alpha)$ fig 10 demonstrates good agreement with X-43 in-flight test and wind tunnel experiments.

The developed software was used for the design of aerodynamic configuration (selection of c.g. location, tail area, and its location, etc.).

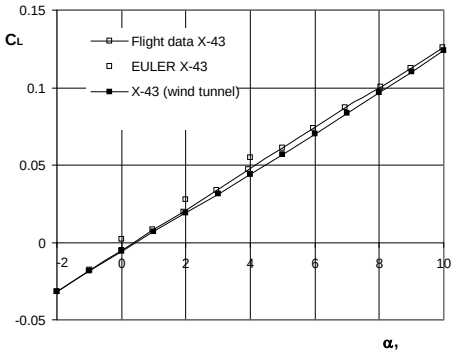

Fig. 9

The model for estimation of thrust force with taking into account the inner part of engine model.

The calculation of the thrust force required to realize a number of intermediate investigations:

- To develop of solid-state model of engine with inner part including inlet and mash around

vehicle body, inlet and inner part of engine (chamber).
- To solve of Navier-Stokes-Fourier equations with turbulence and propulsion model for definition of the gas thermodynamic parameters and fields of velocities:
- To define masses G_{1i}, impulses (longitudinal and lateral) G_{2i}, and G_{3i} and energies of flows $G_{4/i}$ at the input and output of each i-section of the engine;
- To define the thrust T as the difference between impulses of flows at input and output of the engine;
- To calculate the approximation $T = f(H,V,\varphi,a)$

Where φ - combustion efficiency,

a - excess air coefficient

The approximation of $T = f(H,V,\varphi,a)$ was define in two stages. At the first stage the parameters of the airflow at the nose part of the vehicle were defined by the averaging of the Navier-Stokes-Fourier equations. These results allowed to calculate the flow of pulsed impulses and energy through the air gap intake and the longitudinal force acting at the nose part of inlet. The engine thrust was defined on the basis of simplified model of ramjet functioning based on the law of energy conservation, some assumptions on the physical qualities of fuel, turning process, and regime of engine functioning. At the second stage of investigation the developed dependence of thrust was modified by numerical simulation of flow inside multisection part of engine with tacking into account the turbulence and fuel tirning.

The results of calculations are the dependences $T(a,\alpha)$ and $a = f(\alpha)$ for the different combustion efficiency are shown on fig 10.

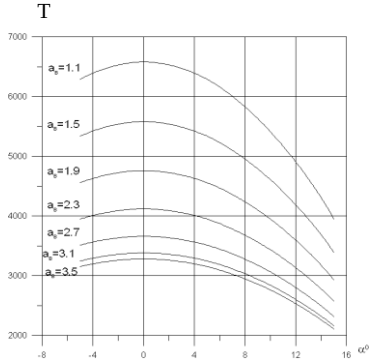

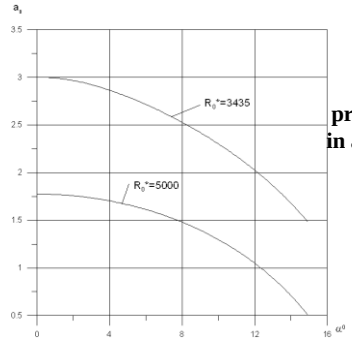

The dependence a=f(α) provides the constant thrust in all range of angle of attack

Fig. 10 Dependence $T = f(a,\alpha)$

The dependence $a = f(\alpha)$ provides the constant thrust in all range of angle of attack.
The influence of thrust on aerodynamic characteristic. In particular it was shown that the change of thrust on ±1% leads to the change of lift force coefficient up to ±5÷7% and to the change of pitch coefficient up to ±15÷25%.
All these results were applied to the flight control system (FCS) design.

2 The HSV flight control system design

The following requirements were tacking into account in the FCS design:

- Accuracy in tracking of command signal, i_{com};
- Suppression of turbulence and wind gusts, d;
- Limitation of required deflection of control surface ($\delta \le \delta_{\max}$);
- Suppression of uncertainties in aerodynamic and thrust characteristics, possible failure (robustness);
- Adaptation to uncertainties and failures.

Two approaches to FCS design were used: traditional and neural network.

2.1 The traditional approach is based on frequency response theory

Two principles were offered in the frame of this approach:

-Series connection of the loops with controllers W_i used the integral laws $W_i = K_i \dfrac{s + \dfrac{1}{T_i}}{s}$ in each of them fig 11. Here W_c is the controlled element dynamic contained the pitch rate loop.

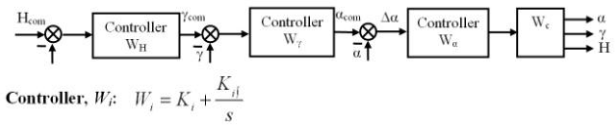

Fig. 11 Series connection of the loops

The integral law was selected because it allows to suppress the uncertainties, nonlinearities and variability in flight control system. As an example, the frequency response characteristics for the open loop $W_{OL}(j\omega) = \dfrac{\alpha(j\omega)}{\Delta\alpha(j\omega)}$ and closed loop system $\dfrac{\alpha(j\omega)}{\alpha_{com}(j\omega)}$ with controllers $W_i = K_i \dfrac{s + \dfrac{1}{T_i}}{s}$ are shown on fig 12, 13 for the different angles of attack. The use if integral law allows to suppress the considerable influence of angle of attack on open loop frequency response characteristics.

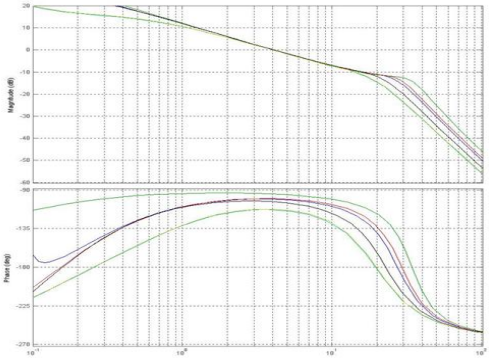

Fig. 12 Open loop frequency response HSV $\dfrac{\alpha(j\omega)}{\Delta\alpha(j\omega)}$

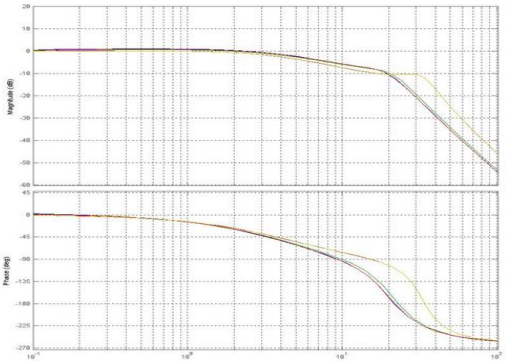

Fig.13 Closed loop frequency response HSV $\dfrac{\alpha(j\omega)}{\alpha_{com}(j\omega)}$

- limitation of derivatives of command signals in each channel and in addition the limitation of maximum and minimum angle of attack in angle of attack loop (fig. 14)

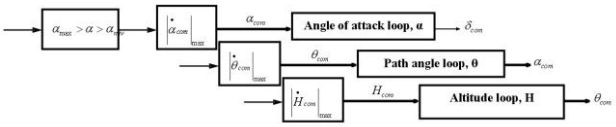

Fig. 14 Limitation of derivatives of command signals

The values of limitations $(\dot{\alpha}_{cam})_{\min}$, $(\dot{\gamma}_{cam})_{\max}$, $(\dot{H}_{cam})_{\max}$ were selected with taking into account to suppress the overshot of the time response $\alpha(t)$. The results shown on fig 15. demonstrate that the developed technique allowed to get the accepted results and provide the considerable decrease of required rate limit (from 350 ^{0}/sec up to 50 ^{0}/sec)

2.2 In the frame of second approach

In the frame of second approach the several versions of adaptive flight control system FCS were investigated. Two of them are considered below.

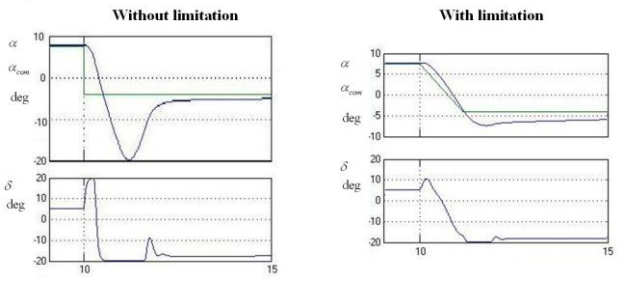

Fig. 16 Influence of the derivatives emits on dynamics response

An application of traditional control theory requires the knowledge of exact plant mathematical model as well as values of plant and environment parameters and characteristics. These requirements can be satisfied not always in practice. Besides it values of plant parameters and its characteristics can be changed in the process of its operation, due to equipment failures or airframe damages, for example. Traditional control theory methods lead often to unacceptable results in that case.

Because of such situation a demand arises to build control systems which do not require full a priori knowledge about the plant and its environment. These systems must afford to adjust themselves to changing conditions including plant and environment properties. Adaptive systems satisfy such demand. They use current available information not only to generate control actions just as it occurs in traditional control systems but to correct a control law.

There are numerous adaptive control schemes including ANN-based ones [8]–[10]. The MRAC (Model Reference Adaptive Control) and MPC (Model Predictive Control) schemes belong to the most frequently used ones (see Figures 17 and 18 respectively).

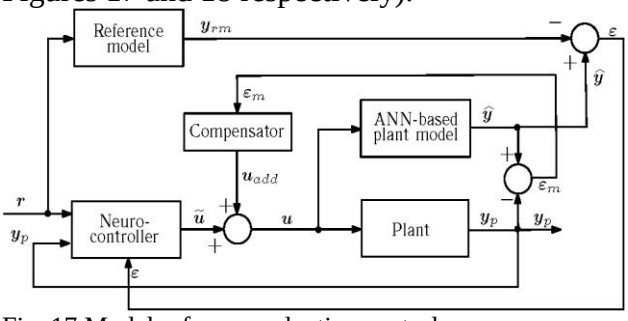

Fig. 17 Model reference adaptive control

General scheme for a model reference adaptive control is shown on Fig. 17. Here $r(t)$ is a reference signal; $y_p(t)$ is a plant output; $y(t)$ is an output of the ANN-model; $y_{rm}(t)$ is a reference model output; $u^*(t)$ control signal generating by neurocontroller; $u_{\text{add}}(t)$ is additional control signal generated with a compensator; $u(t)$ is combined control input acting on the plant; $\varepsilon(t) = y_p(t) - y_m(t)$ is a difference between output of plant and reference model.

A controller in the MRAC scheme can be implemented basing on an artificial neural network. A learning process for the ANN-based controller named below as neurocontroller is accomplished to satisfy proximity condition for motions realized with the reference model and the plant under synthesized control law. The reference model shows an idea of control system designer about "good" or appropriate behavior of the plant which need to be tracked with the neurocontroller.

The ANN-based plant model is used to implement learning process for the neurocontroller. The adjustment purpose specified for the neurocontroller consists in minimization of the error $y_{rm} - y$. In other words it is needed to bring the plant under neurocontroller behavior nearer as possible to the reference model behavior. If the ANN-based model has appropriate accuracy then the neurocontroller will minimize "genuine" error $y_{rm} - y$ too, i.e. it will try to reduce a difference between behavior of the ANN-based plant model and the real plant under the same neurocontroller actions.

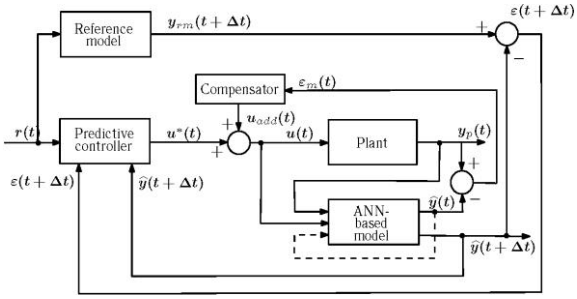

Fig. 18 Model predictive control

The MPC scheme is shown on fig. 17. Here $r(t)$ is a reference signal; $y_p(t)$ is a plant output; $y(t)$ is an output of the ANN-model; $y_{rm}(t)$ is a reference model output; $u^*(t)$ control signal generating by predictive controller based on optimization algorithm; $u_{\text{add}}(t)$ is additional control signal generated with

a compensator; $u(t)$ is combined control input acting on the plant; $\varepsilon(t) = y_p(t) - y_m(t)$ is a difference between outputs of plant and reference model. In this scheme a plant model used to predict future behavior of the plant together with some optimization algorithm to choose appropriate control actions providing best values of predicted characteristics for the considered system.

We have considered MRAC and MPC schemes as applies to control HSV longitudinal short-period motion. Simulation results for those schemes presented demonstrated that the both flight control systems gave the acceptable time response characteristics.

The unique features of adaptive FCS are their potentialities to suppress the uncertainties in aerodynamic and engine characteristics and effects of FCS failure or airframe damage.

The effect of potentialities to adapt the parameters and FCS law of the considered approach is demonstrated on fig. 18

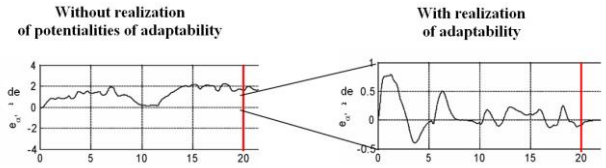

Fig. 18 Influence of adaptability of FCS

It is seen that realization of adaptability in the frame of the considered approach allows to decrease the error of tracking up to 20 times in flight at atmosphere turbulence.

The simulation results of comparison of traditional and adaptive FCS demonstrated that in case of low level of uncertainties these two types of FCS gave the close performance. As for the high level of uncertainties the adaptive FCS has not alternative.

References

[1] Jh. D. Shanghnessy et al *Hypersonic Vehicle Simulation* NASA TM 102610 Nov 1990.

[2] D.Doman et al *Approximate Feedback Linearization of an air-breathings hypersonic Vehicle* AIAA Paper 2004-2012, 2004.

[3] Ch. Marrison and R. Stensel *Design of Robust Control System for a hypersonic aircraft*.

[4] Scott Holland et al *Hyper-X Research Vehicle Experimental aerodynamics Test Program overview*. Journal of Spacecraft and Rockets, Dec 2001

[5] McRuer et *Aeroservoelastic Stabilization techniques for hypersonic Flight vehicles* NASA CR 187617, 1991

[6] Sach G et al *New longitudinal handling qualities criterion for unstable hypersonic vehicles*. AIAA – 2003-5309, 2003

[7] Efremov A.V. *The problems in aerodynamics and flight dynamics of high speed vehicle and ways for their solution.* Proceedings of International Symposium on Hypersonic Aerothermodynamics, India, Bangalore, 2012

[8] A. Astolfi, D. Karagiannis, and R. Ortega. *Nonlinear and adaptive control with applications*. Berlin a.o.: Springer, 2008, 290 pp.

[9] G. Tao *Adaptive control design and analysis*. John Wiley & Sons, Inc., 2003, 618 pp.

[10] P.A. Ioannou and J. Sun *Robust adaptive control*. Prentice Hall, 1995, 848 pp.

Contact Author Email Address

pvl@mai.ru

Copyright Statement